JOC The Journal of Organic Chemistry

Article

pubs.acs.org/joc

Mechanism and Selectivity in Rhodium-Catalyzed [7 + 2] Cycloaddition and Cyclopropanation/Cyclization of Allenylcyclopentane-alkynes: Metallacycle-Directed C(sp^3)-C(sp^3) vs C(sp^3)-H Activation

Genping Huang*

Department of Chemistry, School of Science, Tianjin University, Tianjin 300072, P. R. China

Supporting Information

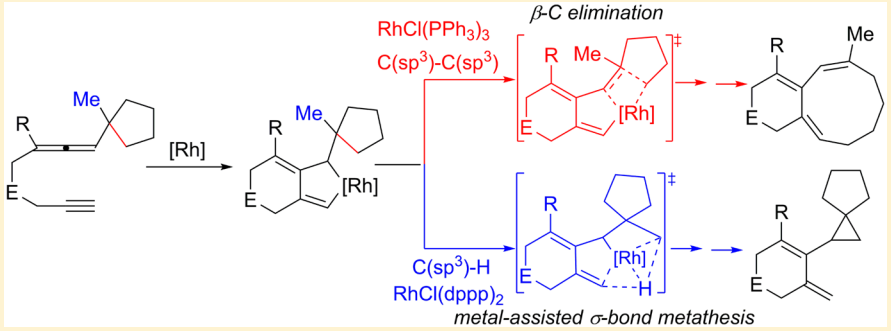

ABSTRACT: The rhodium-catalyzed [7 + 2] cycloaddition and cyclopropanation/cyclization of allenylcyclopentane-alkynes developed by Mukai and co-workers (*J. Am. Chem. Soc.* **2012**, *134*, 19580−19583) represents a rare example of the metallacycle-directed selective C(sp^3)-C(sp^3) vs C(sp^3)-H activation. In this article, the mechanism of this intriguing reaction is investigated by means of density functional theory calculations. The calculations show that the reaction is initiated by an oxidative cyclization to form the key rhodacycle intermediate. The subsequent competing β-carbon elimination/C(sp^3)-C(sp^2) reductive elimination and metal-assisted σ-bond metathesis/C(sp^3)-C(sp^3) reductive elimination lead to the [7 + 2] cycloaddition and cyclopropanation/cyclization, respectively. The calculations reproduce quite well the experimentally observed ligand-controlled selectivity, showing that both electronic and steric effects of the ligand have an important impact on the selectivity. In particular, the ligand can significantly affect energy barriers of the metal-assisted σ-bond metathesis and C−C reductive elimination but toward opposite directions, resulting in a selectivity switch between the [7 + 2] cycloaddition and cyclopropanation/cyclization upon ligand change.

1. INTRODUCTION

Metallacycles are important intermediates in a variety of catalytic processes, widely used both in industry and academia.[1,2] For examples, the oligomerization of olefins, cycloadditions, olefin metathesis, and multicomponent couplings are suggested to proceed through metallacycles.[1,2] Because of the importance of metallacycles, the study of their properties and reactivities has attracted tremendous interest from both experimental[1,2] and theoretical[3,4] chemists. Established reactivities of metallacycles include C−C reductive elimination, migratory insertion, transmetalation, α-hydrogen elimination, and β-hydrogen elimination.[1,2] However, new kinds of reactivities are still emerging,[5] increasing the complexity of mechanistic scenarios involving these intermediates. In this sense, a deeper comprehension of these new reactivities of metallacycles will not only give a better understanding of the already developed transformations but also provide important tools for the design of new processes.

Metallacycles are commonly proposed as key intermediates in transition-metal catalyzed cycloaddition reactions.[2] In this context, Mukai and co-workers recently reported a novel Rh-catalyzed [7 + 2] cycloaddition and cyclopropanation/cyclization of allenylcyclopentane-alkynes (Scheme 1).[6] In this reaction, a metallacycle intermediate was proposed to play a key role, being able to selectively evolve through direct C(sp^3)-C(sp^3) or C(sp^3)-H activations. In particular, when $RhCl(PPh_3)_3$ was used as the catalyst, the reaction undergoes an unprecedented C(sp^3)-C(sp^3) activation to form the [7 + 2] cycloaddition product **2**. Although transition-metal-catalyzed cycloaddition reactions employing cyclopropanes[2a−d] and cyclobutanes[7] have been developed, the analogous reaction occurring on cyclopentanes was considered to be difficult because of the much smaller ring strain energy of cyclopentanes compared to that of cyclopropanes and cyclobutanes.[8] This

Received: May 22, 2015
Published: July 16, 2015

DOI: 10.1021/acs.joc.5b01148
J. Org. Chem. 2015, 80, 7564−7571

Scheme 1. Rh-Catalyzed [7 + 2] Cycloaddition and Cyclopropanation/Cyclization of Allenylcyclopentane-alkynes[a]

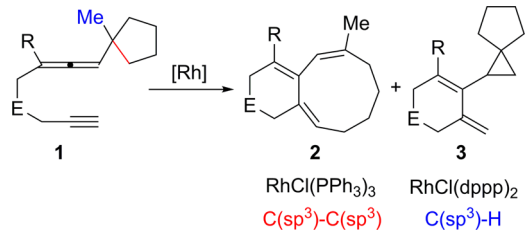

[a]E = $C(CO_2Me)_2$, NTs, $C(CH_2OH)_2$, and etc. R = SO_2Ph; and dppp = 1,3-Bis(diphenylphosphino)propane.[6].

thus represents the first example of a reaction making use of cyclopentane as an acyclic C_5-buliding block in a cycloaddition process. More interestingly, when the catalyst changed to $RhCl(dppp)_2$, the selectivity was switched, and the reaction takes place through a $C(sp^3)$-H activation to afford a novel cyclopropanation/cyclization product **3**.

The Rh-catalyzed cycloadditions of vinylcyclopropanes with unsaturated compounds (e.g., alkynes, alkenes, and allenes) have been extensively investigated computationally, and the reactions were found to be initiated by a C−C cleavage of the cyclopropane.[4] However, for the current reaction, Mukai and co-workers proposed that it first goes through an oxidative cyclization to form the rhodacycle intermediate **A** (Scheme 2). This intermediate **A** then undergoes a $C(sp^3)$-$C(sp^3)$ activation via the β-carbon elimination transition state **B-1**, which would generate the intermediate **C**. Finally, a $C(sp^3)$-$C(sp^2)$ reductive elimination from the intermediate **C** leads to the formation of the [7 + 2] cycloaddition product **2**. Alternatively, a $C(sp^3)$-H activation via the σ-bond metathesis transition state **B-2** was suggested to account for the cyclopropanation/cyclization. The resulting intermediate of the transition state **B-2** is **D**, which then would undergo a $C(sp^2)$-H reductive elimination to get the cyclopropanation/cyclization product **3**.

Very recently, we[9] reported a computational study of the rhodium-catalyzed cyclopropanation/cyclization of allenynes developed by Onoishi and co-workers,[10] which is very relevant to the title reaction. In that work, we have found that instead of the proposed σ-bond metathesis/C−H reductive elimination, the cyclopropanation proceeds through metal-assisted σ-bond metathesis[11] followed by a C−C reductive elimination. With continuous interest in this field and the current poor understanding of the detailed reaction mechanism, in particular the origins of the ligand-controlled $C(sp^3)$-$C(sp^3)$ versus $C(sp^3)$-H activation, we therefore decided to investigate the title reaction computationally by means of density functional theory (DFT) calculations. The present calculations indeed show that our proposed $C(sp^3)$-H activation pathway is much more favorable than the originally proposed one, which provides further corroboration with our previous findings. More importantly, the ligand effect on the metal-assisted σ-bond metathesis/C−C reductive elimination was found to play an important role in determining the selectivity of the reaction.

2. COMPUTATIONAL DETAILS

All of the calculations were performed with the Gaussian 09 package.[12] The geometry optimizations were carried out using the B3LYP functional[13] with the LANL2DZ pseudopotential[14] for Rh, and the 6-31G(d,p) basis set for all other atoms. Frequencies were computed analytically at the same level of theory to confirm whether the structures are minima (no imaginary frequencies) or transition states (only one imaginary frequency). Solvation effects (toluene, ε = 2.3741) were taken into account by performing single-point calculations with the polarizable continuum model (PCM),[15] and the atomic radii used for the PCM calculations were specified using the UFF keyword. Selected transition-state structures were confirmed to connect the correct reactants and products by intrinsic reaction coordinate (IRC) calculations.[16] To obtain better accuracy, single-point energies for the optimized geometries were recalculated with a larger basis set (LANL2TZ(f) for Rh and 6-311+G(d,p) for all other atoms) by using the dispersion-corrected double hybrid functional B2PLYP-D3,[17] which has been demonstrated to yield accurate kinetic and thermodynamic properties.[18] The final free energies reported in the article (ΔG_{Tol}) are the B2PLYP-D3 single-point energies corrected by gas-phase Gibbs free energy correction (at 298.15 K) and solvation correction.

3. RESULTS AND DISCUSSION

The model reaction chosen in the current study is shown in Scheme 3. The experimental results showed that for the

Scheme 3. Model Reaction Investigated in the Current Study

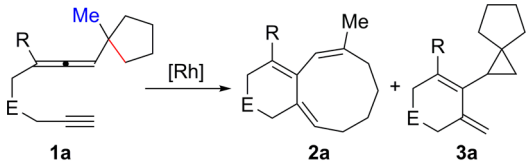

Scheme 2. Originally Proposed Reaction Mechanism[6]

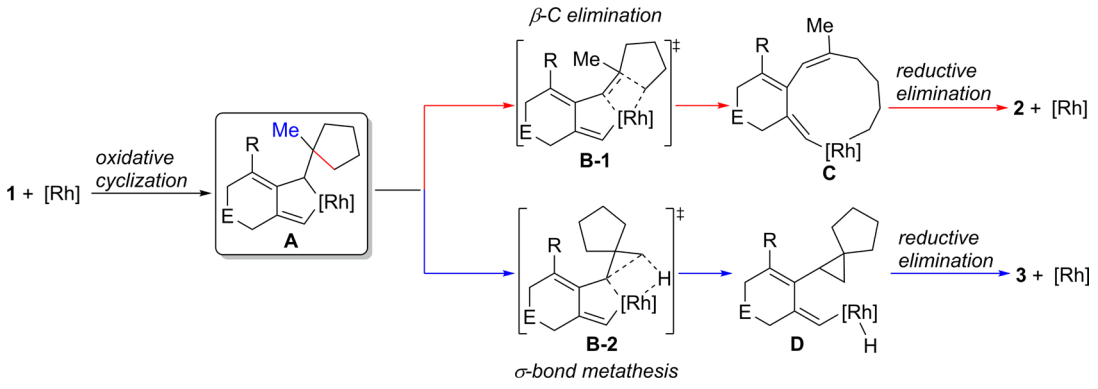

DOI: 10.1021/acs.joc.5b01148
J. Org. Chem. 2015, 80, 7564−7571

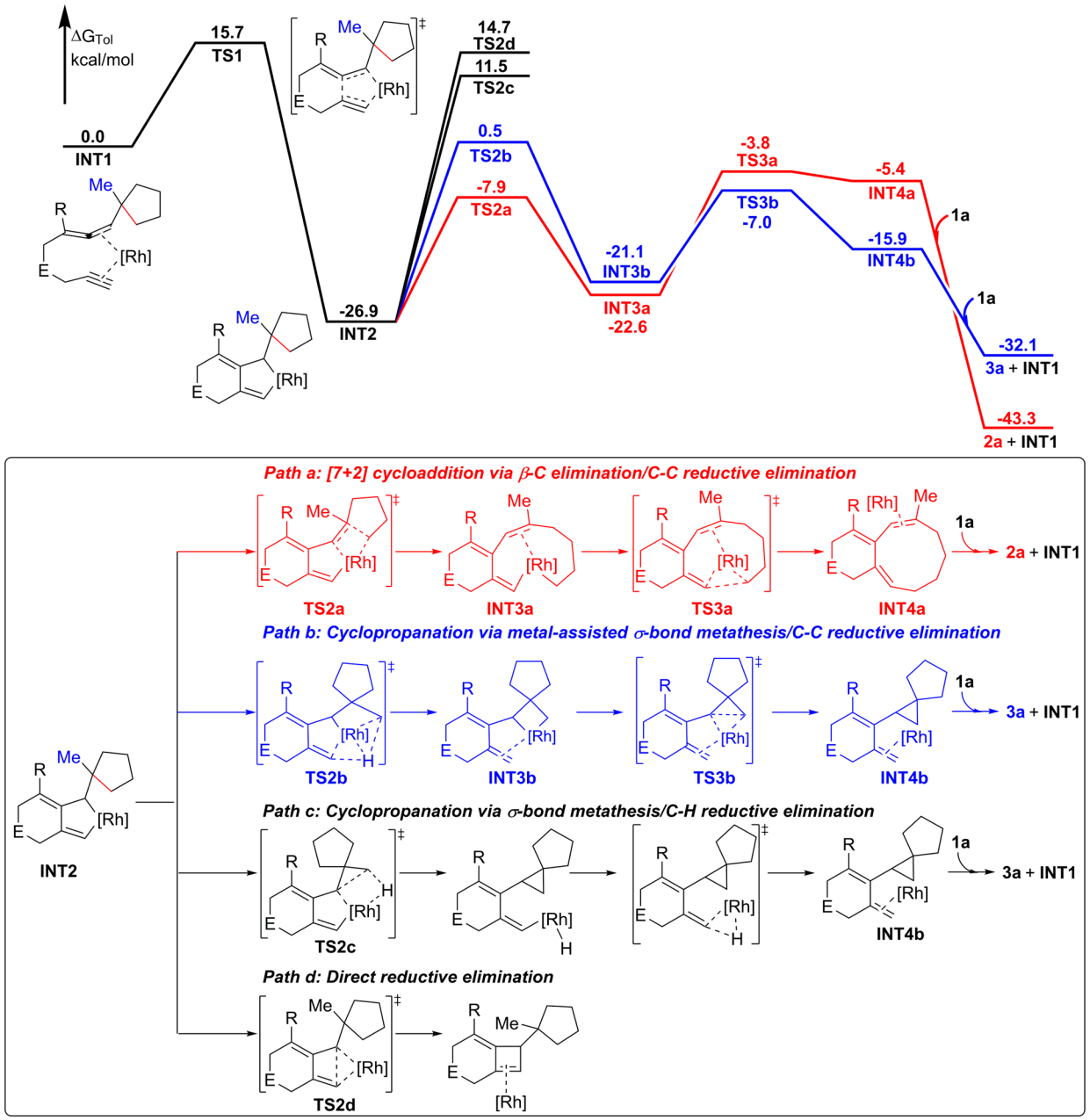

Figure 1. Calculated free energy profiles for the $RhCl(PPh_3)_3$-catalyzed reaction; [Rh] = $RhCl(PPh_3)$.

substrate **1a**, when using the $RhCl(PPh_3)_3$ as catalyst, the [7 + 2] cycloaddition product **2a** was obtained predominantly with a small amount of the cyclopropanation/cyclization product **3a**. However, **3a** was observed as the major product in a 16:1 ratio (**3a**:**2a**) by changing the catalyst to $RhCl(dppp)_2$.

In this section, the results obtained for the $RhCl(PPh_3)_3$-catalyzed reaction are presented first. All possible pathways including the potential side reactions were calculated and compared in order to establish the detailed reaction mechanism. Next, the results of the $RhCl(dppp)_2$-catalyzed reaction are presented. Finally, the origins of the ligand-controlled selectivity are discussed and rationalized on the basis of the calculations.

3.1. Results for the $RhCl(PPh_3)_3$-Catalyzed Reaction. According to Scheme 2, the first step of the reaction is the oxidative cyclization, which was found to initiate from the intermediate **INT1**.[19,20] The calculations show that the oxidative cyclization via **TS1**, involving the distal double bond of the allene and the alkyne moieties, requires an energy barrier of 15.7 kcal/mol with respect to **INT1**, from which the key rhodacyclopentane intermediate **INT2** was generated. This step was calculated to be highly exergonic, by as much as 26.9 kcal/mol. The oxidative cyclization involving the proximal double bond of the allene moiety was also calculated, but the free energy of the corresponding transition state was found to be 12.6 kcal/mol higher than that of **TS1** (see the Supporting Information for details). Considering that the oxidative cyclization is irreversible (*vide infra*), it thus constitutes the first selectivity-determining step of the reaction. The calculations are therefore consistent with the experimental evidence that only the products formed by the cyclization of the distal double bond of the allene were observed.[6] Note that besides the oxidative cyclization, in principle the reaction could also be initiated by the C−C bond cleavage of the cyclopentane

DOI: 10.1021/acs.joc.5b01148
J. Org. Chem. 2015, 80, 7564−7571

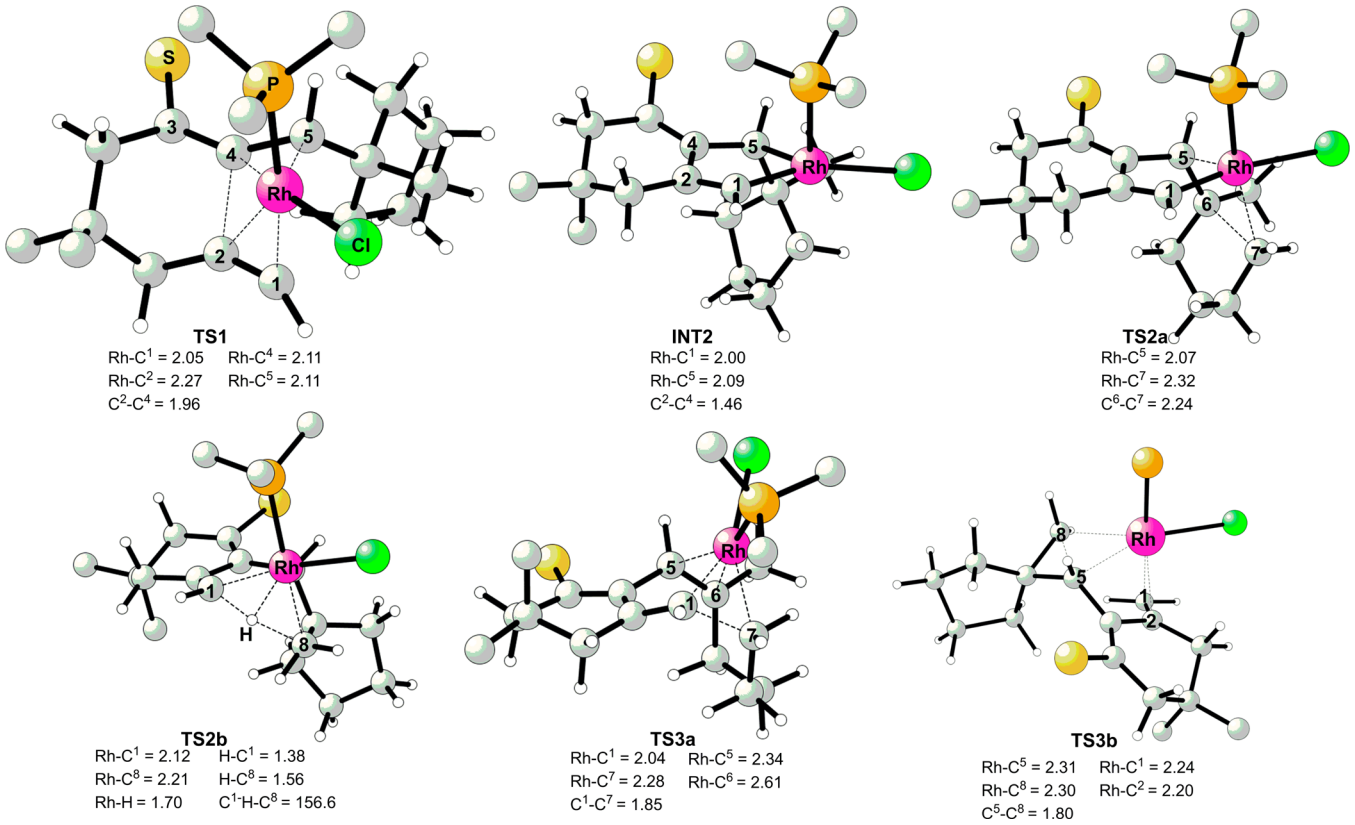

Figure 2. Optimized geometric structures of selected transition states and intermediates in the $RhCl(PPh_3)_3$-catalyzed reaction; the CO_2Me and SO_2Ph groups of **1a** and PPh_3 groups of the ligand were omitted for clarity; distances and angles are in Ångstroms and degrees, respectively.

moiety, similarly to what has been proposed in a number of Rh(I)-catalyzed cycloadditions involving vinylcyclopropanes.[4] However, the calculated energy barrier of this pathway is inaccessibly high (39.0 kcal/mol relative to **INT1**, 23.3 kcal/mol higher than **TS1**), thus ruling out this possibility (see the Supporting Information for details). One possible explanation for this high energy barrier can be found in the difference in strain energy, which is 27.5 kcal/mol for cyclopropanes but only 6.2 kcal/mol for cyclopentanes.[8]

Upon the formation of **INT2**, several mechanistic possibilities can be envisioned, i.e., $C(sp^3)$-$C(sp^3)$ activation via β-carbon elimination, $C(sp^3)$-H activation through σ-bond metathesis, and direct reductive elimination. Path a represents the [7 + 2] cycloaddition occurring through β-carbon elimination/C−C reductive elimination (Figure 1). It was found that the β-carbon elimination takes place via transition state **TS2a**, with an energy barrier of 19.0 kcal/mol relative to **INT2**. The β-carbon elimination was calculated to be endergonic, and the resultant intermediate **INT3a** is 4.3 kcal/mol higher in energy than **INT2**. Subsequently, the intermediate **INT3a** undergoes a $C(sp^3)$-$C(sp^2)$ reductive elimination through **TS3a** to generate the product coordinated intermediate **INT4a**. This step has an energy barrier of 18.8 kcal/mol relative to **INT3a**, i.e., 23.1 kcal/mol relative to **INT2**. Finally, the [7 + 2] cycloaddition is completed by a ligand exchange between the intermediate **INT4a** and the substrate **1a**, which releases the product **2a** and regenerates the intermediate **INT1** for the next catalytic cycle. The overall [7 + 2] cycloaddition was calculated to be highly exergonic, by as much as 43.3 kcal/mol, and the $C(sp^3)$-$C(sp^2)$ reductive elimination (**TS3a**) was found to be the rate-determining step with an overall energy barrier of 23.1 kcal/mol.

Alternatively, the intermediate **INT2** can undergo a $C(sp^3)$-H activation to afford the cyclopropanation/cyclization product **3a**. We first explored the proposed stepwise mechanism, namely, the σ-bond metathesis/C−H reductive elimination (Scheme2). This pathway was found to occur first via transition state **TS2c** (path c, Figure1). However, the energy barrier was calculated to be relatively high, 38.4 kcal/mol relative to **INT2**, which is 19.4 kcal/mol higher than **TS2a**. However, our previously proposed metal-assisted σ-bond metathesis/C−C reductive elimination[9] (path b, Figure 1) was found to be much more favorable than the σ-bond metathesis/C−H reductive elimination. The calculated energy barrier for the metal-assisted σ-bond metathesis via transition state **TS2b** is 27.4 kcal/mol relative to **INT2**, which is lower than that of **TS2c** by as much as 11.0 kcal/mol. In **TS2b** (Figure 2), the hydrogen of the methyl group was directly transferred to the C^1 atom ($H-C^1$ = 1.38 Å, $H-C^8$ = 1.56 Å), with the assistance of the strong interaction between the Rh center and the hydrogen (Rh−H = 1.70 Å). In the meantime, the $Rh-C^1$ bond is breaking and the $Rh-C^8$ bond is forming ($Rh-C^1$ = 2.12 Å, $Rh-C^8$ = 2.21 Å). **TS2b** thus displays geometric features quite similar to those of the transition state obtained in our previous study.[9] The intermediate resulting from **TS2b** is **INT3b**, which was calculated to be 5.8 kcal/mol higher in energy than **INT2**. The $C(sp^3)$-$C(sp^3)$ reductive elimination (**TS3b**) from **INT3b** was found to be relative facile, with an energy barrier of 14.1 kcal/mol relative to that of **INT3b**, i.e., 19.9 kcal/mol relative to **INT2**. To close the catalytic cycle, the cyclopropanation/cyclization product **3a** was released, and **INT1** was regenerated

DOI: 10.1021/acs.joc.5b01148
J. Org. Chem. 2015, 80, 7564−7571

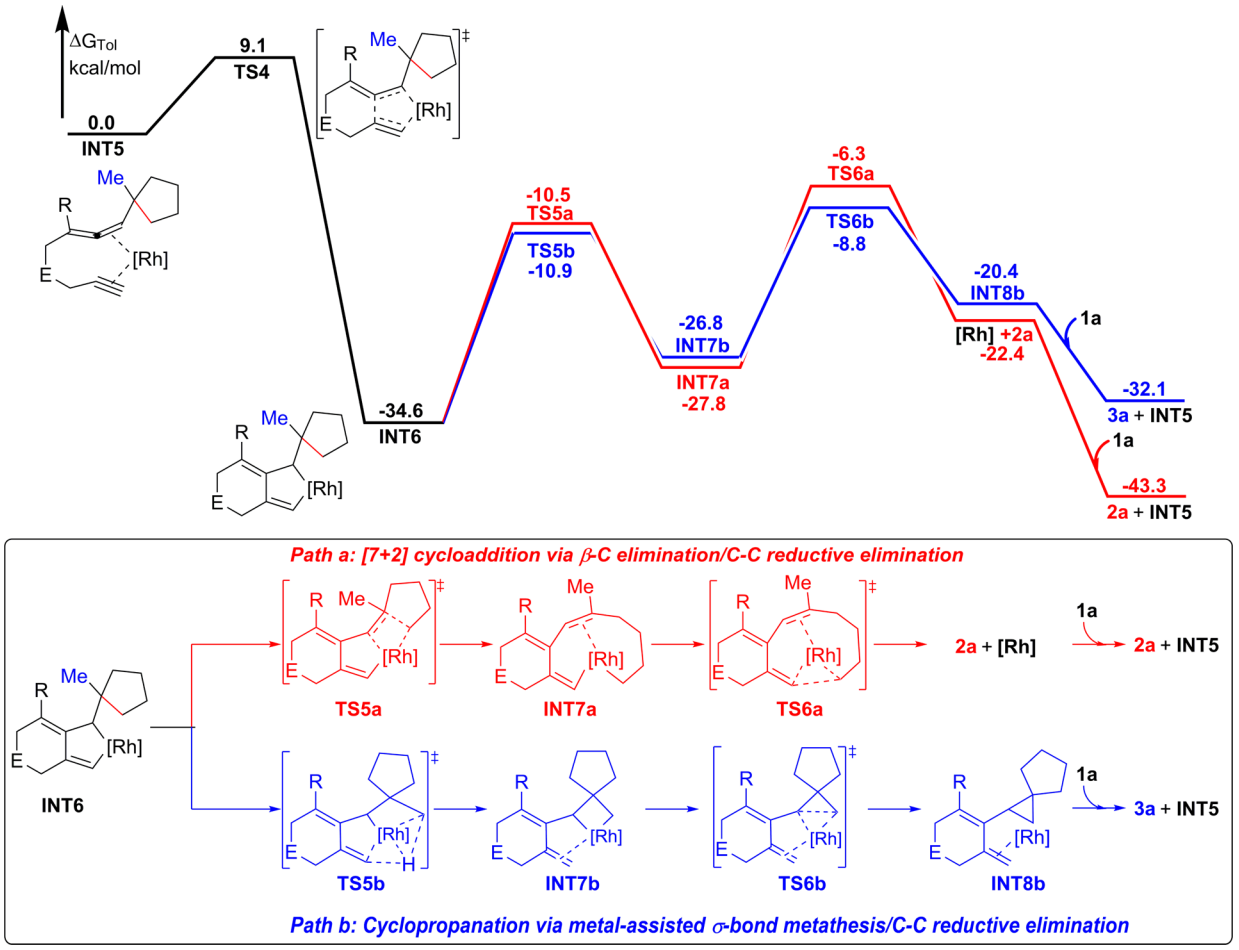

Figure 3. Calculated free energy profiles for the $RhCl(dppp)_2$-catalyzed reaction; [Rh] = RhCl(dppp).

by a ligand exchange step between **INT4b** and **1a**. In short, the rate-determining step of the cyclopropanation/cyclization is the metal-assisted σ-bond metathesis (**TS2b**) with an energy barrier of 27.4 kcal/mol, and the overall reaction is exergonic by 32.1 kcal/mol.

As a final option, we also considered a possible direct C−C reductive elimination from **INT2**. This process would give the [2 + 2] cycloaddition product, which was not experimentally observed. Indeed, the energy barrier for the direct C−C reductive elimination (via **TS 2d**) was calculated to be 41.6 kcal/mol relative to that of **INT2** (path d, Figure 1), which is 18.5 and 14.2 kcal/mol higher than those of the [7 + 2] cycloaddition and the cyclopropanation/cyclization, respectively. This finding is consistent with the experimental results.[6]

Taken together, these results clearly show that the [7 + 2] cycloaddition is the most favorable pathway with an energy barrier of 23.1 kcal/mol. The calculated energy difference of 4.3 kcal/mol between the [7 + 2] cycloaddition and the cyclopropanation/cyclization is in qualitative agreement with the experimental results that the reaction predominantly generated **2a** with a small amount of **3a**.[6] The source of the selectivity lies in the unfavorable metal-assisted σ-bond metathesis step in the cyclopropanation/cyclization compared to that of the [7 + 2] cycloaddition. In the next section, the ligand effect on these elementary steps is presented.

3.2. Results for the $RhCl(dppp)_2$-Catalyzed Reaction.

As mentioned in the Introduction, the selectivity of the reaction was switched from the [7 + 2] cycloaddition to the cyclopropanation/cyclization by changing the catalyst from $RhCl(PPh_3)_3$ to $RhCl(dppp)_2$.[6] In order to elucidate the origins of this ligand-controlled selectivity, the $RhCl(dppp)_2$-catalyzed reaction was investigated. The calculated results are shown in Figure 3, and the optimized geometric structures of selected transition states and intermediates are collected in Figure 4. It turns out that the reaction follows the same general mechanistic pathways as established above for the $RhCl(PPh_3)_3$-catalyzed reaction. However, there are considerable differences in the free energy profiles for the two reactions (Figure 1 vs 3), leading to significant alteration of the reaction selectivity upon ligand change.

Also in this case, the reaction is initiated by an oxidative cyclization (via **TS4**) to form the rhodacyclopentane intermediate **INT6**. This step was found to be very facile, with an energy barrier of only 9.1 kcal/mol relative to that of **INT5**. This barrier is 6.6 kcal/mol lower in energy than the corresponding one found in the $RhCl(PPh_3)_3$-catalyzed reaction (**TS1**), which can be rationalized by recognizing that a more electron-rich ligand, such as dppp, can significantly stabilize an oxidative cyclization transition state.[3a]

As a bifurcation point of the reaction, the intermediate **INT6** can undergo either a β-carbon elimination/$C(sp^3)$-$C(sp^2)$ reductive elimination leading to [7 + 2] cycloaddition (path a, Figure 3) or a metal-assisted σ-bond metathesis/$C(sp^3)$-$C(sp^3)$ reductive elimination, affording the cyclopropanation/cyclization product (path b, Figure 3).[21,22] However, in contrast to the $RhCl(PPh_3)_3$-catalyzed reaction, in which the metal-

DOI: 10.1021/acs.joc.5b01148
J. Org. Chem. 2015, 80, 7564−7571

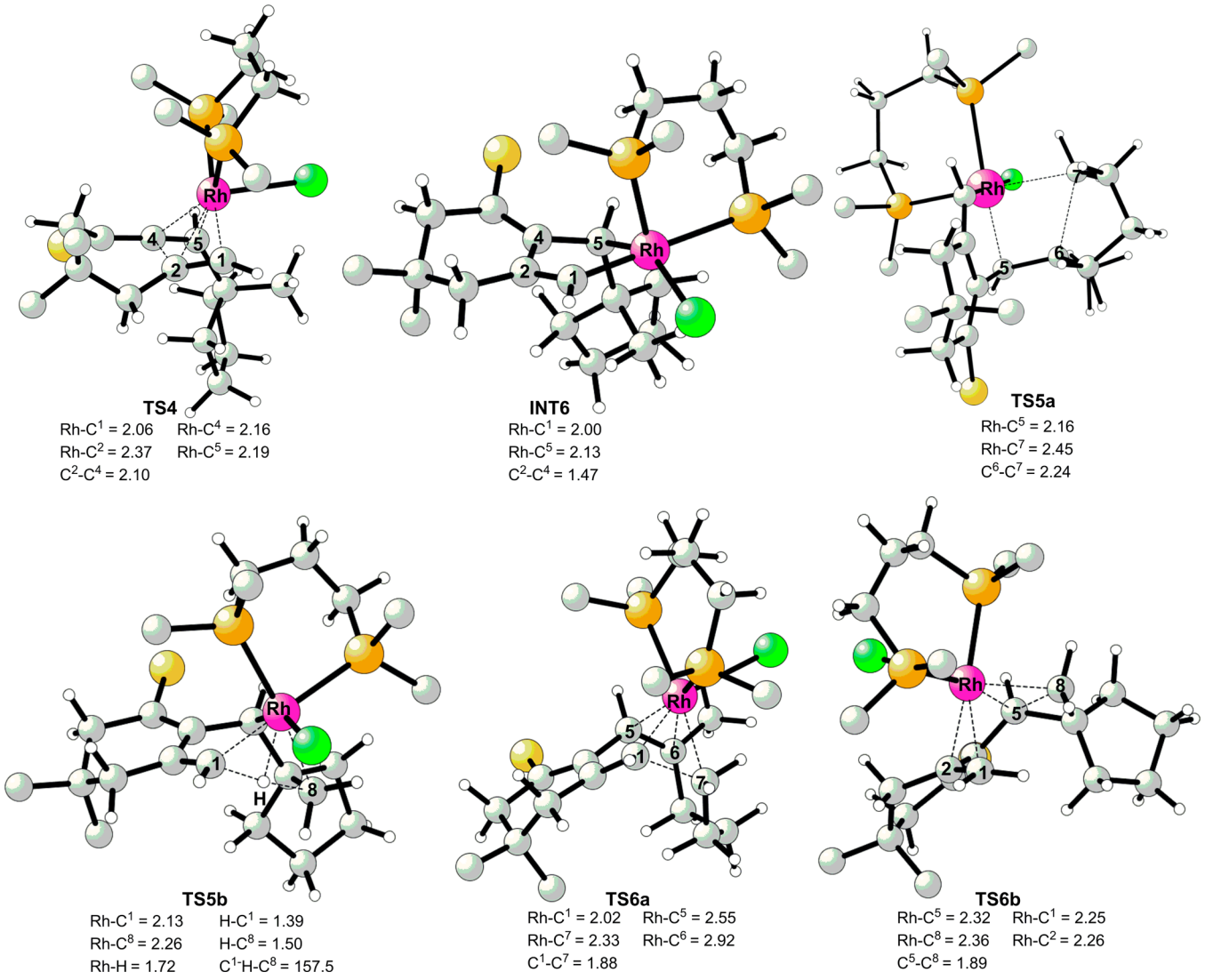

Figure 4. Optimized geometric structures of selected transition states and intermediates in the $RhCl(dppp)_2$-catalyzed reaction.

assisted σ-bond metathesis step is much higher than the β-carbon elimination, and constitutes the rate-determining step for the cyclopropanation/cyclization (Figure 1), for the $RhCl(dppp)_2$-catalyzed reaction the metal-assisted σ-bond metathesis step (via **TS5b**) was calculated to be 0.4 kcal/mol lower than that of the β-carbon elimination (via **TS5a**). Also, more importantly, the $C(sp^3)$-$C(sp^3)$ reductive elimination (via **TS6b**) becomes the rate-determining step. As a consequence, the selectivity of the $RhCl(dppp)_2$-catalyzed reaction is determined by the competition between the C−C reductive elimination in both pathways (**TS6a** vs **TS6b**, Figure 3). The 2.5 kcal/mol energy difference between **TS6a** and **TS6b** implies that the corresponding ratio of **3a**:**2a** is approximately 26:1,[23] in good agreement with the experimental−observed ratio of 16:1.[6] Our results thus clearly reproduce the shift in reaction selectivity from the favorable formation of the [7 + 2] cycloaddition product **2a** in the $RhCl(PPh_3)_3$ case to the preferential formation of the cyclopropanation/cyclization product **3a** in the $RhCl(dppp)_2$-catalyzed reaction.

3.3. Origins of the Ligand-Controlled Selectivity. The origins of the ligand-controlled selectivity are rather complicated, and both electronic and steric effects were found to play important roles in determining the selectivity. For the metal-assisted σ-bond metathesis step, it was found that the energy barrier is 27.4 kcal/mol for the $RhCl(PPh_3)_3$ case (**TS2b**), while 23.7 kcal/mol for the $RhCl(dppp)_2$ (**TS5b**). Given that more steric repulsion is present in **TS2b** than in **TS5b**, the difference in the electronic properties between PPh_3 and dppp ligands therefore determines the reactivity of this step. Previous studies have shown that the C−H activation via σ-bond metathesis is most likely involving a degree of heterolytic character, which thus can be viewed as a proton transfer. Moreover, the transition state can be stabilized with more electron-rich metal center.[24] In this sense, the Rh center with the more electron-rich dppp ligand in the current case therefore can significantly stabilize the metal-assisted σ-bond metathesis. The NBO analysis shows that the transferring hydrogen has a significant amount of positive charge in both **TS2b** (+0.294*e*) and **TS5b** (+0.314*e*). Moreover, the Rh center in **TS5b** displays a much more negative charge than that in **TS2b** (−0.493e vs −0.129*e*). These results indeed corroborate well with the previous arguments.

However, the β-carbon elimination and C−C reductive elimination were found to be more sensitive to steric effect. The calculations show that the energy barriers for β-carbon elimination and C−C reductive elimination were increased by

DOI: 10.1021/acs.joc.5b01148
J. Org. Chem. 2015, 80, 7564−7571

about 5−6 kcal/mol when changing the ligand from PPh_3 to dppp (Figures 1 and 3). Comparison of the geometric structures further supports that the steric repulsion between the catalyst and the substrate moieties plays an important role in these steps. Taking **TS2a** and **TS5a** as examples, the bond distances of Rh−C^5 and Rh−C^7 in **TS2a** are 2.07 and 2.32 Å, respectively, while they are 2.16 and 2.45 Å, respectively, in **TS5a** (Figures 2 and 4). Besides the steric effect, it should also be mentioned that the C−C reductive elimination should be more favored with the PPh_3 ligand than with the more electron-rich dppp ligand.

Finally, in the current study the C(sp^3)-C(sp^3) reductive elimination was found to take place inherently more easily than the C(sp^3)-C(sp^2) reductive elimination, with an energy difference of ca. 3 kcal/mol, regardless of the ligand employed in the reaction. The reason for this is that in the C(sp^3)-C(sp^3) reductive elimination, the rhodium center is coordinated by the external C^1−C^2 double bond, while in the C(sp^3)-C(sp^2) reductive elimination the metal is coordinated by the internal C^5−C^6 double bond. The latter coordination is less favorable due to the higher steric repulsion.

Therefore, the electronic and steric effects of the ligand combined together enable a selectivity switch upon the ligand change. Moreover, the ligand effect on the metal-assisted σ-bond metathesis and C−C reductive elimination was found to point toward the opposite directions. In other words, the Rh catalyst with the dppp ligand can easily promote the metal-assisted σ-bond metathesis step due to the electronic effect but does not favor the C−C reductive elimination because of both the effects. As a result, the selectivity is determined by the C−C reductive elimination, leading to the cyclopropanation/cyclization. The Rh catalyst with the PPh_3 ligand shows an unfavorable metal-assisted σ-bond metathesis but with relatively easy C−C reductive elimination. This results in the selectivity being determined by the competition between the C(sp^3)-C(sp^2) reductive elimination and the metal-assisted σ-bond metathesis, with the formation of the [7 + 2] cycloaddition product.

4. CONCLUSIONS

In the current study, the rhodium-catalyzed [7 + 2] cycloaddition and cyclopropanation/cyclization of allenylcyclopentane-alkynes was investigated by means of DFT calculations. The calculations indicate that the reaction is initiated by an oxidative cyclization to form a rhodacyclopentane intermediate. The subsequent β-carbon elimination and a C(sp^3)-C(sp^2) reductive elimination led to the [7 + 2] cycloaddition product, while a metal-assisted σ-bond metathesis and a C(sp^3)-C(sp^3) reductive elimination led to the cyclopropanation/cyclization product.

The calculations reproduce quite well the experimentally observed ligand-controlled selectivity. Both electronic and steric effects of the ligand were found to play important roles in determining the selectivity. For the $RhCl(PPh_3)_3$-catalyzed reaction, it was shown that the selectivity originates from the unfavorable metal-assisted σ-bond metathesis compared to that of the C(sp^3)-C(sp^2) reductive elimination of the [7 + 2] cycloaddition. For the $RhCl(dppp)_2$-catalyzed reaction, it turns out that the Rh center with the more electron-rich dppp ligand can significantly enhance the metal-assisted σ-bond metathesis but does not favor the C−C reductive elimination due to electronic and steric effects. This leads to the selectivity being determined by the competing C−C reductive elimination, resulting in a selectivity change from the [7 + 2] cycloaddition to the cyclopropanation/cyclization. Therefore, the ligand has a significant impact on both the metal-assisted σ-bond metathesis and C−C reductive elimination but toward opposite directions, which combined together enables a selectivity switch upon the ligand change.

The present calculations provide thus a number of new insights into the metallacycle-directed C−C and C−H activations, which should have important implications for the design of new catalytic systems.

■ ASSOCIATED CONTENT

Supporting Information

Additional computational results, table of calculated energies, and Cartesian coordinates of all optimized structures. The Supporting Information is available free of charge on the ACS Publications website at DOI: 10.1021/acs.joc.5b01148.

■ AUTHOR INFORMATION

Corresponding Author

*E-mail: gphuang@tju.edu.cn; Web: http://genpinghuang.weebly.com.

Notes

The authors declare no competing financial interest.

■ ACKNOWLEDGMENTS

We thank Professor Zhi-Xiang Wang and Dr. Stefano Santoro for valuable discussions. Computer time was generously provided by the High Performance Computing Center of Tianjin University, P. R. China.

■ REFERENCES

(1) For selected reviews, see: (a) Fürstner, A. *Angew. Chem., Int. Ed.* **2000**, *39*, 3012−3043. (b) Zheng, F.; Sivaramakrishna, A.; Moss, J. R. *Coord. Chem. Rev.* **2007**, *251*, 2056−2071. (c) McGuinness, D. S. *Chem. Rev.* **2011**, *111*, 2321−2341. (d) Blom, B.; Clayton, H.; Kilkenny, M.; Moss, J. R. *Adv. Organomet. Chem.* **2006**, *54*, 149−201. (e) Albrecht, M. *Chem. Rev.* **2010**, *110*, 576−623. (f) Ng, S.-S.; Ho, C.-Y.; Schleicher, K. D.; Jamison, T. F. *Pure Appl. Chem.* **2008**, *80*, 929−939. (g) Tasker, S. Z.; Standley, E. A.; Jamison, T. F. *Nature* **2014**, *509*, 299−309. (h) Tanaka, K.; Tajima, Y. *Eur. J. Org. Chem.* **2012**, *2012*, 3715−3725. (i) Standley, E. A.; Tasker, S. Z.; Jensen, K. L.; Jamison, T. F. *Acc. Chem. Res.* **2015**, *48*, 1503−1514. (j) Gandeepan, P.; Cheng, C.-H. *Acc. Chem. Res.* **2015**, *48*, 1194−1206.

(2) For selected reviews on the transition metal-catalyzed cycloadditions, see: (a) Wender, P. A.; Gamber, G. G.; Williams, T. J. In *Modern Rhodium-Catalyzed Organic Reactions*; Evans, P. A., Ed.; Wiley-VCH: Weinheim, Germany, 2005; pp 263−299. (b) Pellissier, H. *Adv. Synth. Catal.* **2011**, *353*, 189−218. (c) Jiao, L.; Yu, Z.-X. *J. Org. Chem.* **2013**, *78*, 6842−6848. (d) Gao, Y.; Fu, X.-F.; Yu, Z.-X. *Top. Curr. Chem.* **2014**, *346*, 195−231. (e) Ylijoki, K. E.O.; Stryker, J. M. *Chem. Rev.* **2013**, *113*, 2244−2266. (f) Wender, P. A. *Tetrahedron* **2013**, *69*, 7529−7550. (g) Schienebeck, C. M.; Li, X.; Shu, X.-Z.; Tang, W. *Pure Appl. Chem.* **2014**, *86*, 409−417. (h) Pellissier, H.; Clavier, H. *Chem. Rev.* **2014**, *114*, 2775−2823. (i) Shibata, Y.; Tanaka, K. *Synthesis* **2012**, *44*, 323−350. (j) Broere, D. L. J.; Rujiter, E. *Synthesis* **2012**, *44*, 2639−2672. (k) Nakamura, I.; Yamamoto, Y. *Chem. Rev.* **2004**, *104*, 2127−2198. (l) Amatore, M.; Aubert, C. *Eur. J. Org. Chem.* **2015**, *2015*, 265−286. (m) Inglesby, P. A.; Evans, P. A. *Chem. Soc. Rev.* **2010**, *39*, 2791−2805. (n) Yamamoto, Y. *Chem. Rev.* **2012**, *112*, 4736−4769. (o) Aubert, C.; Buisine, O.; Malacria, M. *Chem. Rev.* **2002**, *102*, 813−834. (p) Aubert, C.; Fensterbank, L.; Garcia, P.; Malacria, M.; Simonneau, A. *Chem. Rev.* **2011**, *111*, 1954−1993.

(3) For selected examples, see: (a) Hong, X.; Liu, P.; Houk, K. N. *J. Am. Chem. Soc.* **2013**, *135*, 1456−1462. (b) Hong, X.; Trost, B. M.;

DOI: 10.1021/acs.joc.5b01148
J. Org. Chem. 2015, 80, 7564−7571

Houk, K. N. *J. Am. Chem. Soc.* **2013**, *135*, 6588−6600. (c) Dang, Y.; Qu, S.; Tao, Y.; Song, C.; Wang, Z.-X. *J. Org. Chem.* **2014**, *79*, 9046−9064. (d) Huang, G.; Kalek, M.; Himo, F. *J. Am. Chem. Soc.* **2013**, *135*, 7647−7659. (e) Xu, L.; Zhu, Q.; Huang, G.; Cheng, B.; Xia, Y. *J. Org. Chem.* **2012**, *77*, 3017−3024. (f) Williams, V. M.; Kong, J. R.; Ko, B. J.; Mantri, Y.; Brodbelt, J. S.; Baik, M.-H.; Krische, M. J. *J. Am. Chem. Soc.* **2009**, *131*, 16054−16062. (g) Mazumder, S.; Shang, D.; Negru, D. E.; Baik, M.-H.; Evans, P. A. *J. Am. Chem. Soc.* **2012**, *134*, 20569−20572. (h) Liao, W.; Yu, Z.-X. *J. Org. Chem.* **2014**, *79*, 11949−11960.

(4) For selected examples, see: (a) Mustard, T. J. L.; Wender, P. A.; Cheong, P. H.-Y. *ACS Catal.* **2015**, *5*, 1758−1763. (b) Hong, X.; Stevens, M. C.; Liu, P.; Wender, P. A.; Houk, K. N. *J. Am. Chem. Soc.* **2014**, *136*, 17273−17283. (c) Xu, X.; Liu, P.; Lesser, A.; Sirois, L. E.; Wender, P. A.; Houk, K. N. *J. Am. Chem. Soc.* **2012**, *134*, 11012−11025. (d) Lin, M.; Kang, G.-Y.; Guo, Y.-A.; Yu, Z.-X. *J. Am. Chem. Soc.* **2012**, *134*, 398−405. (e) Jiao, L.; Lin, M.; Yu, Z.-X. *J. Am. Chem. Soc.* **2011**, *133*, 447−461. (f) Yu, Z.-X.; Cheong, P. H.-Y.; Liu, P.; Legault, C. Y.; Wender, P. A.; Houk, K. N. *J. Am. Chem. Soc.* **2008**, *130*, 2378−2379. (g) Liu, P.; Cheong, P. H.-Y.; Yu, Z.-X.; Wender, P. A.; Houk, K. N. *Angew. Chem., Int. Ed.* **2008**, *47*, 3939−3941. (h) Yu, Z.-X.; Wender, P. A.; Houk, K. N. *J. Am. Chem. Soc.* **2004**, *126*, 9154−9155. (i) Wang, Y.; Wang, J.; Su, J.; Huang, F.; Jiao, L.; Liang, Y.; Yang, D.; Zhang, S.; Wender, P. A.; Yu, Z.-X. *J. Am. Chem. Soc.* **2007**, *129*, 10060−10061. (j) Liang, Y.; Jiang, X.; Fu, X.-F.; Ye, S.; Wang, T.; Yuan, J.; Wang, Y.; Yu, Z.-X. *Chem. - Asian J.* **2012**, *7*, 593−604.

(5) For selected examples, see: (a) Inglesby, P. A.; Bacsa, J.; Negru, D. E.; Evans, P. A. *Angew. Chem., Int. Ed.* **2014**, *53*, 3952−3956. (b) Yip, S. Y. Y.; Aïssa, C. *Angew. Chem., Int. Ed.* **2015**, *54*, 6870−6873. (c) Ohashi, M.; Kawashima, T.; Taniguchi, T.; Kikushima, K.; Ogoshi, S. *Organometallics* **2015**, *34*, 1604−1607. (d) Kumar, P.; Thakur, A.; Hong, X.; Houk, K. N.; Louie, J. *J. Am. Chem. Soc.* **2014**, *136*, 17844−17851. (e) Feng, J.-J.; Lin, T.-Y.; Wu, H.-H.; Zhang, J. *J. Am. Chem. Soc.* **2015**, *137*, 3787−3790. (f) Noucti, N. N.; Alexanian, E. J. *Angew. Chem., Int. Ed.* **2015**, *54*, 5447−5450. (g) Fu, W.; Nie, M.; Wang, A.; Cao, Z.; Tang, W. *Angew. Chem., Int. Ed.* **2015**, *54*, 2520−2524. (h) Chauvin, Y. *Angew. Chem., Int. Ed.* **2006**, *45*, 3740−3747. (i) Vivancos, Á.; Vattier, F.; López-Serrano, J.; Paneque, M.; Poveda, M. L.; Álvarez, E. *J. Am. Chem. Soc.* **2015**, *137*, 4074−4077. (j) Wang, H.; Negretti, S.; Knauff, A. R.; Montgomery, J. *Org. Lett.* **2015**, *17*, 1493−1496. (k) Chen, J.; Lee, K.-H.; Wen, T.; Gao, F.; Sung, H. H. Y.; Williams, I. D.; Lin, Z.; Jia, G. *Organometallics* **2015**, *34*, 890−896.

(6) Mukai, C.; Ohta, Y.; Oura, Y.; Kawaguchi, Y.; Inagaki, F. *J. Am. Chem. Soc.* **2012**, *134*, 19580−19583.

(7) Inagaki, F.; Sugikubo, K.; Oura, Y.; Mukai, C. *Chem. - Eur. J.* **2011**, *17*, 9062−9065.

(8) (a) Anslyn, E. V.; Dougherty, D. A. *Modern Physical Organic Chemistry*; University Science Books: Sausalito, CA, 2006; pp 100−102. (b) Hong, X.; Liang, Y.; Griffith, A. K.; Lambert, T. H.; Houk, K. N. *Chem. Sci.* **2014**, *5*, 471−475.

(9) Huang, G. *Org. Lett.* **2015**, *17*, 1994−1997.

(10) Oonishi, Y.; Kitano, Y.; Sato, Y. *Angew. Chem., Int. Ed.* **2012**, *51*, 7305−7308.

(11) (a) Vastine, B. A.; Hall, M. B. *J. Am. Chem. Soc.* **2007**, *129*, 12068−12069. (b) Hartwig, J. F.; Cook, K. S.; Hapke, M.; Incarvito, C. D.; Fan, Y.; Webster, C. E.; Hall, M. B. *J. Am. Chem. Soc.* **2005**, *127*, 2538−2552.

(12) Frisch, M. J.; Trucks, G. W.; Schlegel, H. B.; Scuseria, G. E.; Robb, M. A.; Cheeseman, J. R.; Scalmani, G.; Barone, V.; Mennucci, B.; Petersson, G. A.; Nakatsuji, H.; Caricato, M.; Li, X.; Hratchian, H. P.; Izmaylov, A. F.; Bloino, J.; Zheng, G.; Sonnenberg, J. L.; Hada, M.; Ehara, M.; Toyota, K.; Fukuda, R.; Hasegawa, J.; Ishida, M.; Nakajima, T.; Honda, Y.; Kitao, O.; Nakai, H.; Vreven, T.; Montgomery, J. A., Jr.; Peralta, J. E.; Ogliaro, F.; Bearpark, M.; Heyd, J. J.; Brothers, E.; Kudin, K. N.; Staroverov, V. N.; Kobayashi, R.; Normand, J.; Raghavachari, K.; Rendell, A.; Burant, J. C.; Iyengar, S. S.; Tomasi, J.; Cossi, M.; Rega, N.; Millam, M. J.; Klene, M.; Knox, J. E.; Cross, J. B.; Bakken, V.; Adamo, C.; Jaramillo, J.; Gomperts, R.; Stratmann, R. E.; Yazyev, O.; Austin, A. J.; Cammi, R.; Pomelli, C.; Ochterski, J. W.; Martin, R. L.; Morokuma, K.; Zakrzewski, V. G.; Voth, G. A.; Salvador, P.; Dannenberg, J. J.; Dapprich, S.; Daniels, A. D.; Farkas, Ö.; Foresman, J. B.; Ortiz, J. V.; Cioslowski, J.; Fox, D. J. *Gaussian 09*; Gaussian, Inc.: Wallingford, CT, 2010.

(13) (a) Lee, C. T.; Yang, W. T.; Parr, R. G. *Phys. Rev. B: Condens. Matter Mater. Phys.* **1988**, *37*, 785−789. (b) Miehlich, B.; Savin, A.; Stoll, H.; Preuss, H. *Chem. Phys. Lett.* **1989**, *157*, 200−206. (c) Becke, A. D. *J. Chem. Phys.* **1993**, *98*, 5648−5652.

(14) Hay, P. J.; Wadt, W. R. *J. Chem. Phys.* **1985**, *82*, 270−283.

(15) Tomasi, J.; Persico, M. *Chem. Rev.* **1994**, *94*, 2027−2094.

(16) (a) Fukui, K. *J. Phys. Chem.* **1970**, *74*, 4161−4163. (b) Fukui, K. *Acc. Chem. Res.* **1981**, *14*, 363−368.

(17) (a) Grimme, S.; Ehrlich, S.; Goerigk, L. *J. Comput. Chem.* **2011**, *32*, 1456−1465. (b) Grimme, S.; Antony, J.; Ehrlich, S.; Krieg, H. *J. Chem. Phys.* **2010**, *132*, 154104−154119. (c) Goerigk, L.; Grimme, S. *J. Chem. Theory Comput.* **2011**, *7*, 291−309.

(18) For selected examples, see: (a) Wolf, L. M.; Thiel, W. *J. Org. Chem.* **2014**, *79*, 12136−12147. (b) Krenske, E. H.; Petter, R. C.; Zhu, Z.; Houk, K. N. *J. Org. Chem.* **2011**, *76*, 5074−5081. (c) Ciancaleoni, G.; Rampino, S.; Zuccaccia, D.; Tarantelli, F.; Belanzoni, P.; Belpassi, L. *J. Chem. Theory Comput.* **2014**, *10*, 1021−1034. (d) Xue, X.-S.; Li, X.; Yu, A.; Yang, C.; Song, C.; Cheng, J.-P. *J. Am. Chem. Soc.* **2013**, *135*, 7462−7473. (e) Jin, L.; Wu, Y.; Zhao, X. *J. Org. Chem.* **2015**, *80*, 3547−3555.

(19) (a) **INT1** was formed by a ligand exchange step between the substrate **1a** and $RhCl(PPh_3)_3$. Houk and co-workers showed that a similar process is highly exergonic, see: Xu, X.; Liu, P.; Shu, X.-z.; Tang, W.; Houk, K. N. *J. Am. Chem. Soc.* **2013**, *135*, 9271−9274. (b) Other possible complexes formed between **1a** and $RhCl(PPh_3)_3$, e.g., the coordination only with either the alkyne moiety or the double bond of allene moiety, were also considered. However, the free energies were found to be much higher than that of **INT1**.

(20) Previous theoretical studies have suggested the $RhCl(PPh_3)$ as the active species in the $RhCl(PPh_3)_3$-catalyzed cycloaddition reactions, see: (a) Liu, T.; Han, L.; Han, S.; Bi, S. *Organometallics* **2015**, *34*, 280−288. (b) Haraburda, E.; Torres, Ò.; Parella, T.; Solà, M.; Pla-Quintana, A. *Chem. - Eur. J.* **2014**, *20*, 5034−5045. (c) Dachs, A.; Osuna, S.; Roglans, A.; Solà, M. *Organometallics* **2010**, *29*, 562−569 Selected key transition states with two PPh_3 ligands were also tested in our calculations, but the optimizations led to the automatic dissociation of one PPh_3 ligand.

(21) Other possibilities from **INT6** were also calculated, but all of them were found to be associated with very high energy barriers. See the Supporting Information for details.

(22) Key transition states (e.g., **TS5a**, **TS5b**, **TS6a**, and **TS6b**) were also optimized with the monodentate coordination of the dppp ligand. The results show that the energies are much higher than their bidentate counterparts; see the Supporting Information for details.

(23) Considering that the (**3a** + **INT5**) is 2.5 kcal/mol less stable than **INT6**, it is possible that **3a** can convert to the [7 + 2] cycloaddition product **2a**, which is about 11 kcal/mol more stable than **3a**. However, the interconversion between **2a** and **3a** must proceed through the intermediate **INT6**, from which the formation of **3a** is always favored. In addition, from the (**3a** + **INT5**), the forward reaction to the next catalytic cycle is always much more favorable than the backward reaction to **INT6** (9.1 vs 23.3 kcal/mol). Therefore, we conclude that **3a** is the major product.

(24) (a) Lin, Z. *Coord. Chem. Rev.* **2007**, *251*, 2280−2291. (b) Boutadla, Y.; Davies, D. L.; Macgregor, S. A.; Poblador-Bahamonde, A. I. *Dalton Trans.* **2009**, 5820−5831.

DOI: 10.1021/acs.joc.5b01148
J. Org. Chem. 2015, 80, 7564−7571